Available online at www.sciencedirect.com

ScienceDirect

Ceramics International 40 (2014) 4333–4340

CERAMICS INTERNATIONAL

www.elsevier.com/locate/ceramint

Effect of nanocarbon sources on microstructure and mechanical properties of MgO–C refractories

Tianbin Zhu[a], Yawei Li[a,*], Shaobai Sang[a], Shengli Jin[a,b], Yuanbing Li[a], Lei Zhao[a], Xiong Liang[a]

[a]*The Key State Laboratory Breeding Base of Refractories and Ceramics, Wuhan University of Science and Technology, 430081 Wuhan, PR China*
[b]*Chair of Ceramics, University of Leoben, Peter-Tunner-Straße 5, 8700 Leoben, Austria*

Received 7 August 2013; received in revised form 22 August 2013; accepted 22 August 2013
Available online 8 September 2013

Abstract

A study of microstructural evolution, mechanical and thermo-mechanical properties of MgO–C refractories, based on graphite oxide nanosheets (GONs), carbon nanotubes (CNTs) and carbon black (CB), was carried out by means of X-ray diffraction (XRD), scanning electron microscopy (SEM) coupled with energy dispersive X-ray spectroscopy (EDS), three-point bending and thermal shock tests. Meanwhile, these results were compared to the conventional MgO–C refractory containing 10 wt% flaky graphite prepared under the same conditions. The results showed that higher cold modulus of rupture was obtained for the composition containing GONs, and the composition containing CNTs exhibited larger displacement after coking at 1000 °C and 1400 °C. Also, the addition of nanocarbons led to an improvement of the thermal shock resistance; in particular, both compositions containing CNTs and CB had higher residual strength ratio, approaching the thermal shock resistance of the reference composition containing 10 wt% flaky graphite, as it was associated with the presence of nanocarbons and *in-situ* formation of ceramic phases in the matrix.

Keywords: C. Mechanical properties; C. Thermal shock resistance; Nanocarbons; MgO–C refractories

1. Introduction

Thanks to their excellent thermal, chemical and mechanical properties, MgO–C refractories are widely applied in steel-making equipment and components, for instance, converters, electric arc furnaces, RH vacuum degassers and slide gates for the flow control of Ca-treated steel [1–3]. However, conventional MgO–C refractories comprise a high amount of carbon up to 12–18 wt% and thus they are sensitive to the oxidation. Furthermore, high carbon pick-up in molten steel is encountered as well as the high energy loss and emission of CO_x when they are in service [4–6]. In order to satisfy the requirements of advanced steel-making technology and environmental protection, many efforts have been made to develop the low carbon containing refractories recently. The application of nanocarbons in the form of nano-carbon black (CB), carbon nanotubes (CNTs), carbon nanofibers (CNFs), graphene or graphite oxide nanosheets (GONs) shows great potential in developing low carbon containing refractories with enhanced properties. The literature [6–16] reported that developed low carbon MgO–C refractories using CB exhibited better mechanical and thermo-mechanical properties than conventional high carbon MgO–C refractories. Also, Luo et al. [17] found that the addition of CNTs benefited *in-situ* formation of SiC whiskers in the matrix and consequently the mechanical properties of Al_2O_3–C refractories were improved. It was also reported that adding 0.4 wt% CNFs in the MgO–C refractories enhanced the flexural strength by 2.2 times compared to that of specimens without CNFs [18]. In our previous work, GONs were incorporated into MgO–C and Al_2O_3–C refractories, and superior properties were obtained, due to the combination effects of the relatively homogeneous distribution of GONs and *in-situ* formation of ceramic phases interlocked with each other [19–21].

Although the addition of nanocarbons in carbon containing refractories shows improvement on the mechanical properties, the complete replacement of flaky graphite by nanocarbons is a very tough task because the nanocarbons are more prone to oxidation than the flaky graphite. Also, the extensive research is limited on MgO–C refractories utilizing single nanocarbon

*Corresponding author. Tel.: +86 27 68862188; fax: +86 27 68862018.
E-mail addresses: liyawei@wust.edu.cn, liyaweiwust@hotmail.com (Y. Li).

0272-8842/$ - see front matter © 2013 Elsevier Ltd and Techna Group S.r.l. All rights reserved.
http://dx.doi.org/10.1016/j.ceramint.2013.08.101

source, and the effects of various nanocarbon sources on the microstructure and mechanical properties of MgO–C refractories still need to be further explored. Out of the reasons, the present work makes a comparative study of MgO–C refractories using three kinds of nanocarbon sources, respectively. The results are also compared with conventional MgO–C refractory containing 10 wt% flaky graphite (without any nanocarbon) prepared under the same conditions.

2. Experimental

2.1. Preparation of MgO/C composite powders

In order to distribute nanocarbons homogeneously in magnesia powders (~45 μm, 98 wt%, Dashiqiao, China), different MgO/C composite powders were prepared firstly. The preparation method of MgO-GONs was shown in Refs. [19,20]. The MgO-CNTs and MgO-CB composite powders were prepared in the following manner: the as-obtained CNTs (diameter, 20–70 nm; length, ~20 μm; >95.0 wt% fixed carbon; Chengdu, China) or CB (~30 nm, >99.0 wt% fixed carbon, Pingdingshan, China) and MgO powders (~45 μm, 98 wt%, Dashiqiao, China) were mixed manually in a mass ratio of 2:100 respectively and then wet-milled using absolute alcohol as the disperse media at room temperature for 7 h in a planetary ball mill (corundum balls as the abrasive media) with the rotating speed of 400 r/min, in which the ratio of corundum balls to the powder mixtures was 1:1. Afterwards, the composite powders were dried at 60 °C for 48 h followed by grinding.

2.2. Preparation of MgO–C refractory specimens

Fused magnesia (3–1 mm, 1–0.5 mm, 0.5–0 mm and <45 μm, 98 wt% MgO, Dashiqiao, China), metallic aluminum (<45 μm, 98 wt% Al, Xinxiang, China), silicon powder (<45 μm, 98 wt% Si, Anyang, China), flaky graphite (FG, <74 μm, 97.5 wt% fixed carbon, Qingdao, China), and different MgO/C composite powders were used as raw materials. Thermo-setting phenolic resins, one in liquid form (36 wt% of carbon yield, Zibo, China) and one in powder form (55 wt% carbon yield, Zibo, China) were used as binder. Different MgO–C compositions were formulated by varying nanocarbon sources. Conventionally used MgO–C refractory (composition Ref. 2), containing 10 wt% flaky graphite as carbon source, has also been prepared under the same conditions. The investigated MgO–C compositions are presented in Table 1. All the compositions were mixed for 30 min in a mixer with a rotating speed of 80–100 r/min. After kneading, bar shaped specimens ($25 \times 25 \times 140$ mm^3) were compacted under a pressure of 150 MPa and then cured at 200 °C for 24 h. Finally, the as-prepared specimens were treated at a heating rate of 5 °C/min to 1000 °C and 1400 °C for 3 h in a sagger filled with coke grit, respectively.

2.3. Testing and characterization methods

Cold modulus of rupture (CMOR), flexural modulus (FM) and displacement were measured by the three-point bending test at ambient temperature with a span of 100 mm and a loading rate of 0.5 mm/min using an electronic digital control system (EDC 120, DOLI Company, Germany). The force–displacement curve of each specimen was recorded simultaneously during the test. Also, the thermal shock behavior of MgO–C specimens after coking at 1400 °C was determined. The specific method of the thermal shock test was referred to Refs. [19,20].

The crystallographic phases of the coked samples were determined via X-ray diffractometry (XRD) (X'Pert Pro, Philips, Eindhoven, The Netherlands; using Ni filtered, Cu K_α radiation at a scanning rate of 2 deg/min and a temperature of 16 °C). The microstructural evaluation was carried out by means of field emission scanning electron microscopy (FSEM) (Nova 400 Nano FESEM, FEI Co., Philips, Eindhoven, The Netherlands) coupled with energy dispersive X-ray spectroscopy (EDS) (EDAX, Phoenix, Philips, Eindhoven, The Netherlands).

Table 1
Investigated MgO–C compositions.

Raw materials	Compositions (wt%)				
	GN	CT	CB	Ref. 1	Ref. 2
Fused magnesia aggregate	70	70	70	70	70
Magnesia powders	12	12	12	22	17
Flaky graphite	4.8	4.8	4.8	5	10
MgO-GONs	10.2				
MgO-CNTs		10.2			
MgO-CB			10.2		
Silicon powder	1	1	1	1	1
Metallic aluminum	2	2	2	2	2
Phenolic resin powder	+1	+1	+1	+1	+1
Liquid phenolic resin	+4	+4	+4	+4	+4

3. Results and discussion

3.1. SEM images of different MgO/C composite powders

Fig. 1 shows the SEM images of various MgO/C composite powders. Obviously, FG was an irregular and laminated structure (Fig. 1a), and nanocarbons (GONs, CNTs and CB) were distributed rather homogeneously in MgO powders, as shown in Fig. 1b–d, respectively.

3.2. Phase composition and microstructure of MgO–C compositions

XRD analysis of the investigated MgO–C compositions after coking at 1000 °C identified the main phases as periclase, graphite, spinel ($MgAl_2O_4$) and silicon, which were in agreement with those reported by the previous study [19,20,22,23]. The SEM micrographs of the MgO–C compositions after coking at 1000 °C are shown in Fig. 2. All the investigated compositions presented a similar microstructure. Next to the typical *in-situ* formation of $MgAl_2O_4$ grains (Fig. 2a–e), the *in-situ* formed whiskers of Al carbides were also evident

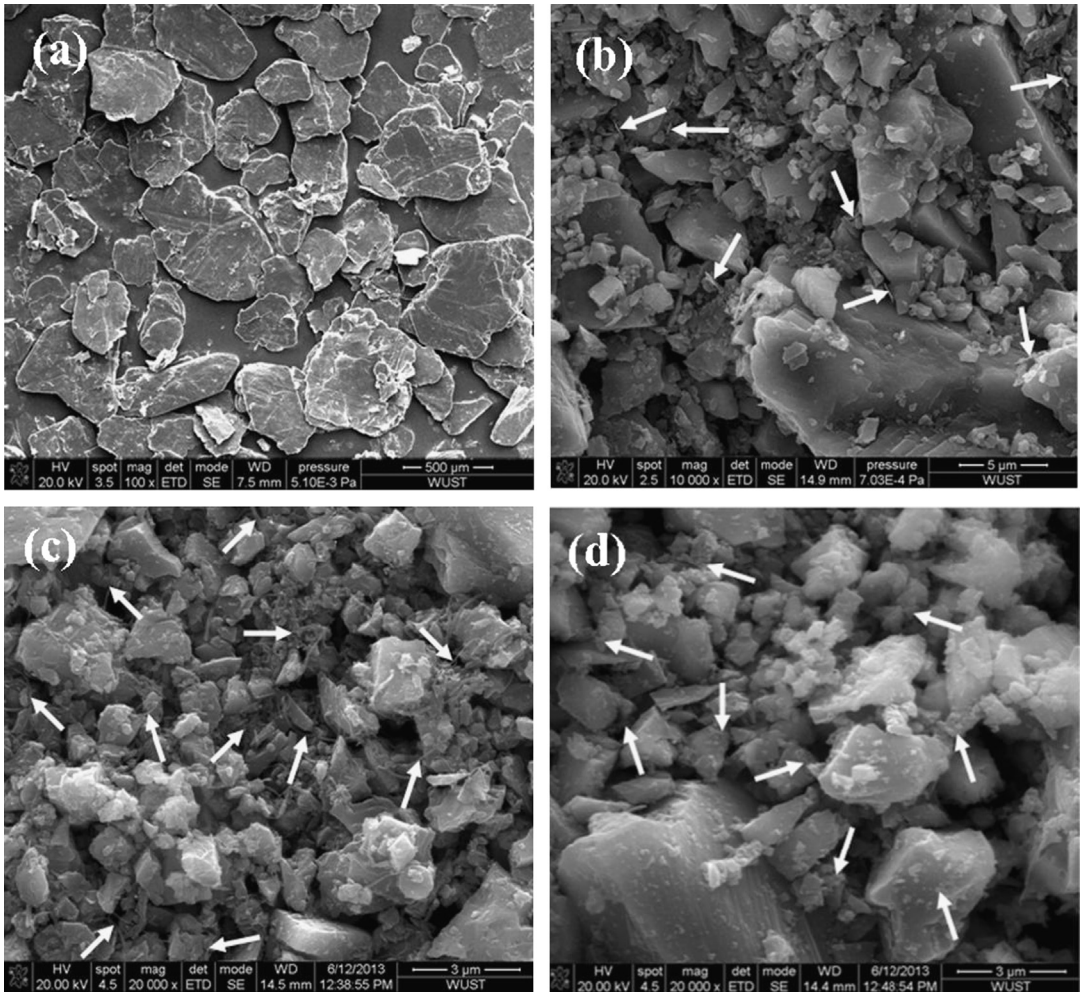

Fig. 1. SEM images of various carbon sources: (a) FG, (b) MgO-GONs, (c) MgO-CNTs, and (d) MgO-CB.

(Fig. 2a–e), which were verified by the EDS analysis. As for their morphology, the whiskers of Al carbides had a diameter of 50–100 nm and a length of up to several micrometers.

In the case of the MgO–C compositions after coking at 1400 °C, XRD analysis also did not present any remarkable differences on the crystallographic phases; the identified phases were periclase, graphite, spinel, AlN and SiC for all the compositions. However, their microstructural evolution during the coking process was different apparently, as shown in Fig. 3. The SEM micrographs of the composition Ref. 2 with 10 wt% flaky graphite revealed the *in-situ* formation of magnesium aluminate spinel crystals in the matrix (Fig. 3a and b), which was confirmed by the EDS analysis. The reduction of the flaky graphite content from 10 wt% to 5 wt% led to a significantly different microstructure of the Ref. 1 composition. Besides the octahedral spinel crystals, the plate-like AlN particles formed at the site where metal Al particles originally occupied (Fig. 3c and d), which was verified by XRD and EDS.

The microstructural evolution of the MgO–C compositions containing various nanocarbons after coking at 1400 °C is displayed in Fig. 3e–j. Compared with the composition Ref. 1, the compositions GN and CT exhibited much more *in-situ* formed plate-like AlN phase in the matrix (Fig. 3e–h). Furthermore, some of residual CNTs were observed at the local area in the composition CT (Fig. 3h), implying that the composition CT may have higher toughness. Surprisingly, the composition CB did not show any plate-like AlN phase but a great number of prismatic AlN (Fig. 3i–j), which was confirmed by the EDS analysis. All these differences of microstructure can be explained by the change of the partial pressure of CO(g) and N_2(g) in the interior portion of refractories. Similar phenomena were also reported in the literature that the *in-situ* formation of different shaped particles or whiskers strongly depended on additives, treating atmospheres, coking temperatures, *etc*. during the experiment [23–25].

3.3. Mechanical properties of MgO–C compositions

The microstructure differences of the MgO–C compositions have a direct impact on their mechanical properties, as shown in Table 2 and Fig. 4. Compared to the composition Ref. 1, the CMOR and FM of the composition Ref. 2 were lower at all the treated temperatures. In the case of the compositions containing nanocarbons, the composition GN showed the

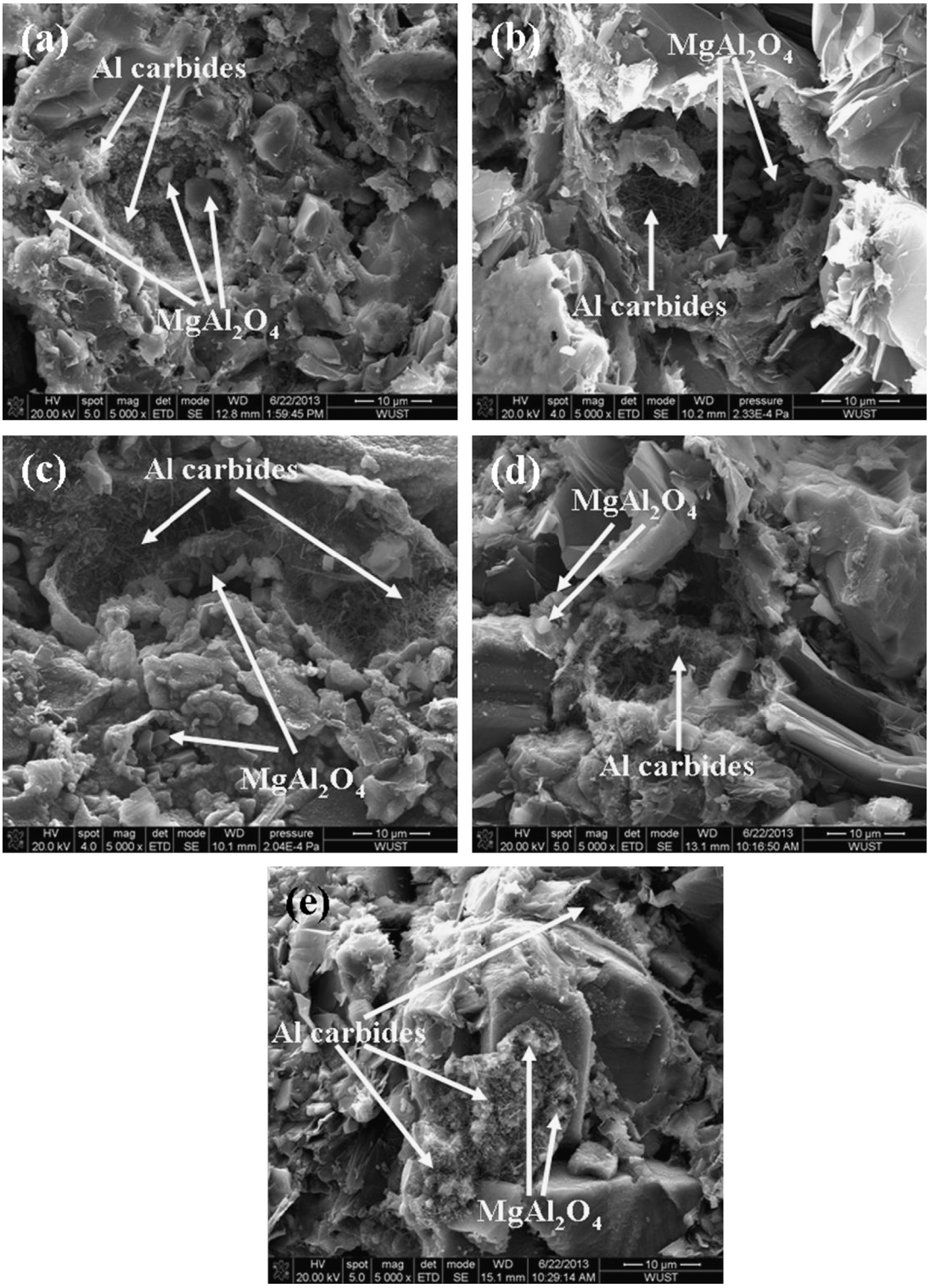

Fig. 2. SEM micrographs of fracture surfaces of MgO–C compositions coked at 1000 °C: (a) Ref. 2, (b) Ref. 1, (c) GN, (d) CT, and (e) CB.

highest CMOR and FM values at all the treated temperatures. As expected, CMOR and FM of all the compositions treated at 200 °C were the highest. However, when the coking temperature was 1000 °C, CMOR and FM of all the compositions decreased sharply due to the pyrolysis of the binder resin. As the coking temperature increasing to 1400 °C, the composition GN had the highest strength, which was related to the amount and morphology of *in-situ* formed ceramic phases in the matrix (Fig. 3).

Fig. 4 shows the force–displacement curves of the investigated MgO–C compositions after treating at different temperatures. Apparently, the changes of force and displacement had the similar tendency with CMOR and FM (Fig. 4 and Table 2). Also, the displacement of the compositions containing nanocarbons was

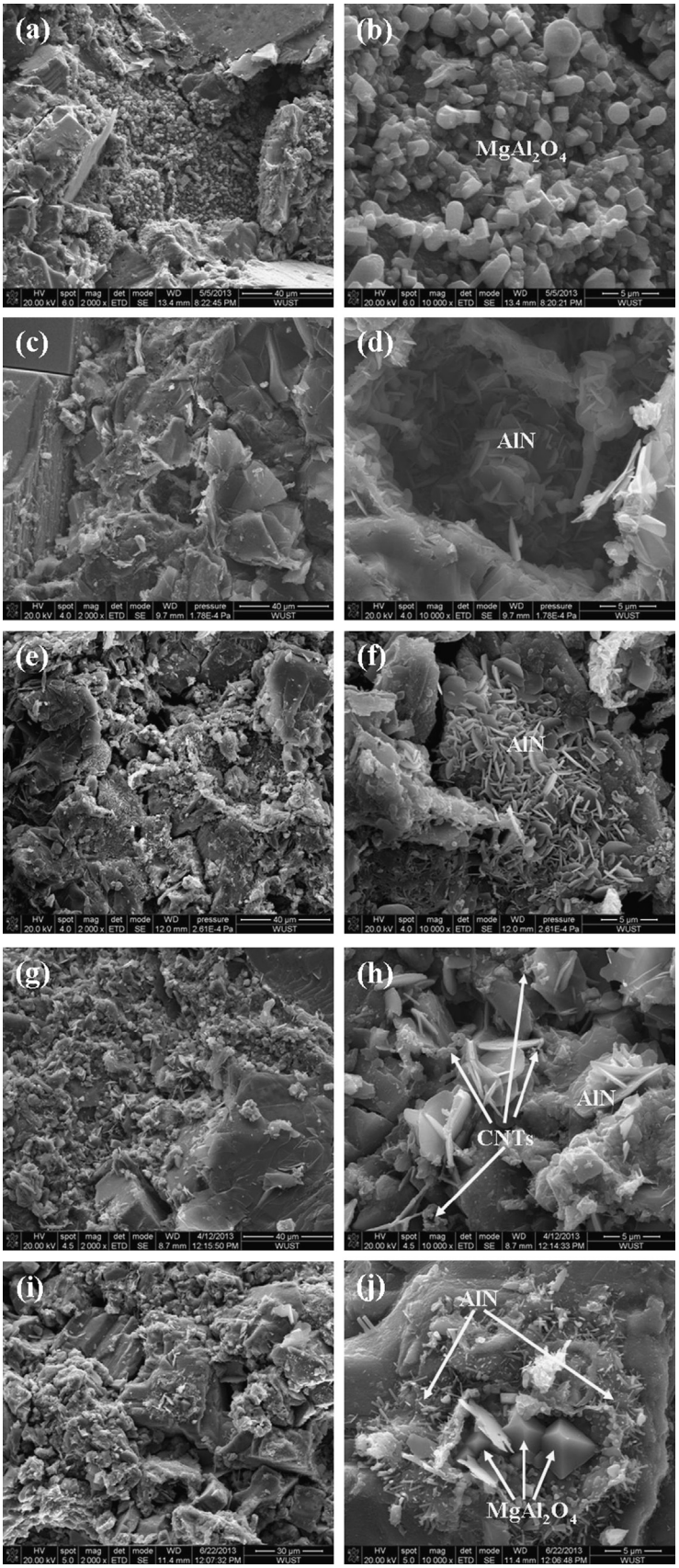

Fig. 3. SEM micrographs of fracture surfaces of MgO–C compositions coked at 1400 °C: (a) and (b) Ref. 2, (c) and (d) Ref. 1, (e) and (f) GN, (g) and (h) CT, and (i) and (j) CB.

Table 2
CMOR, FM and displacement of MgO–C compositions treated at various temperatures.

Temperature	Properties	GN	CT	CB	Ref. 1	Ref. 2
200 °C	CMOR (MPa)	23.96 ± 0.96	18.61 ± 1.21	20.08 ± 1.13	20.33 ± 0.92	19.86 ± 0.75
	FM (GPa)	5.94 ± 0.32	4.82 ± 0.28	5.39 ± 0.45	5.48 ± 0.53	5.16 ± 0.38
	Displacement (mm)	0.54 ± 0.02	0.47 ± 0.01	0.46 ± 0.01	0.44 ± 0.01	0.39 ± 0.02
1000 °C	CMOR (MPa)	7.72 ± 0.12	6.78 ± 0.18	6.29 ± 0.27	6.41 ± 0.22	6.10 ± 0.14
	FM (GPa)	2.26 ± 0.03	2.03 ± 0.02	2.02 ± 0.02	2.14 ± 0.04	2.08 ± 0.03
	Displacement (mm)	0.45 ± 0.01	0.52 ± 0.02	0.46 ± 0.01	0.41 ± 0.01	0.40 ± 0.02
1400 °C	CMOR (MPa)	10.97 ± 0.45	10.28 ± 0.38	9.23 ± 0.32	10.02 ± 0.25	9.84 ± 0.21
	FM (GPa)	2.76 ± 0.07	2.36 ± 0.05	2.30 ± 0.06	2.65 ± 0.09	2.19 ± 0.02
	Displacement (mm)	0.43 ± 0.01	0.46 ± 0.01	0.44 ± 0.01	0.42 ± 0.01	0.39 ± 0.01

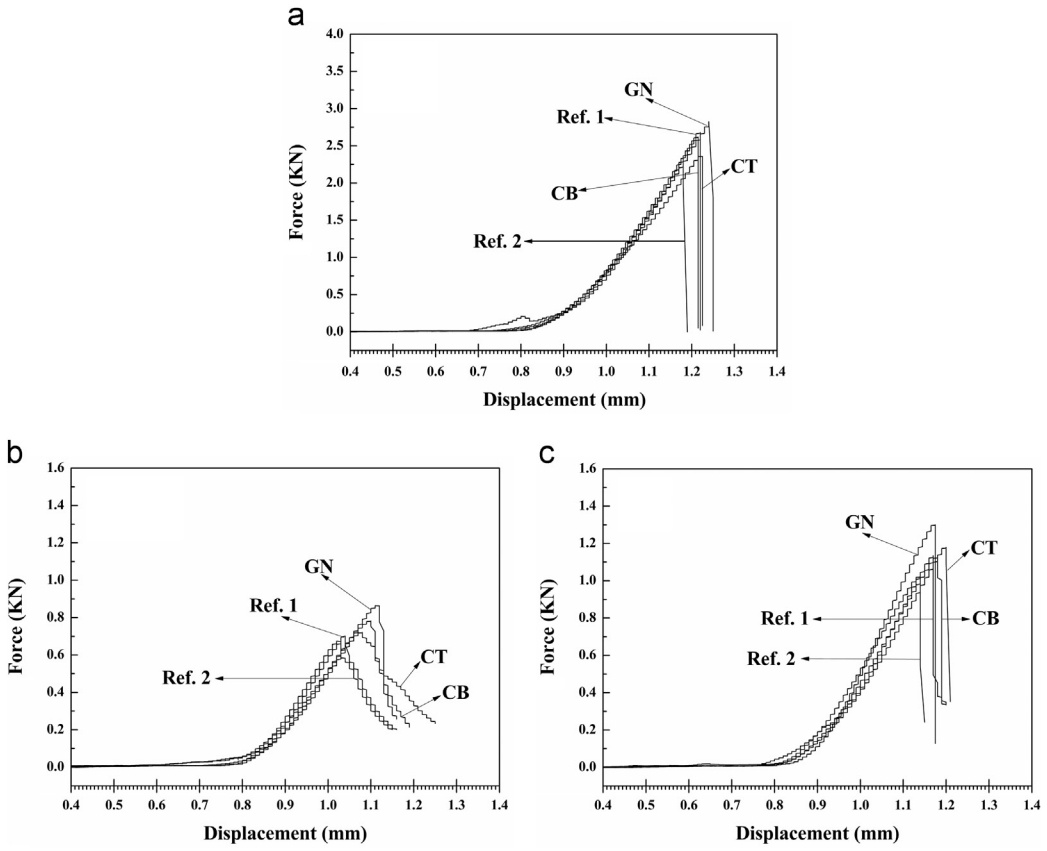

Fig. 4. Force–displacement curves of MgO–C compositions treated at 200 °C (a), 1000 °C (b), and 1400 °C (c).

larger than that of the composition only with flaky graphite for all the treated temperatures. Especially, the composition CT after coking at 1000 °C and 1400 °C manifested the largest displacement, which was attributed to the combination effects of CNTs added and *in-situ* formation of ceramic phases (Fig. 3h).

3.4. Thermal shock resistance of MgO–C compositions

Regarding the thermal shock behavior of the compositions after coking at 1400 °C, expressed by the residual CMOR after 5 thermal shock cycles (named as $CMOR_{TS}$), all the compositions containing nanocarbons exhibited higher residual CMOR and lower strength loss compared to the composition Ref. 1, as shown in Table 3. For instance, the compositions containing nanocarbons (CB, CT and GN) had the residual strength ratio of higher than 40%, but 37.43% for the composition Ref. 1, indicating that the addition of nanocarbons is helpful to the improvement of thermal shock resistance of MgO–C compositions. In particular, the compositions CT and CB had a higher residual CMOR and a lower strength loss after thermal shock, approaching the thermal shock resistance of the composition Ref. 2. It may be suggested that a combination of homogeneous distribution of nanocarbons and microstructural evolution during the coking process decisively contributes to the thermal shock behavior of MgO–C refractories. Many publications have reported that nano-scaled materials can not only

Table 3
The CMOR change of MgO–C compositions coked at 1400 °C after 5 thermal shocks.

	GN	CT	CB	Ref. 1	Ref. 2
CMOR (MPa)	10.97 ± 0.45	10.28 ± 0.38	9.23 ± 0.32	10.02 ± 0.25	9.84 ± 0.21
$CMOR_{TS}$ (MPa)	4.56 ± 0.25	4.85 ± 0.19	4.45 ± 0.23	3.75 ± 0.14	5.29 ± 0.22
The residual strength ratio (5TS) (%)	41.57	47.17	48.21	37.43	53.71

absorb and relieve the stress due to the thermal expansion and shrinkage of refractory particles, but also reduce maldistribution of thermal stress in the interior portion of refractories [26–28], thus improving their thermal shock resistance. In addition, the homogeneous dispersion of nanocarbons may inhibit the sintering of MgO powders and consequently reduces the modulus of elasticity and improves thermal shock resistance.

4. Conclusions

The influence of different nanocarbons (GONs, CNTs and CB) on the microstructure, mechanical and thermal shock resistance of MgO–C refractories were investigated in the present work. The addition of nanocarbons had a positive influence on the *in-situ* formation of ceramic phases with different amounts and morphology after coking at 1000 °C and 1400 °C, thus influencing the mechanical properties and thermal shock resistance of MgO–C refractories. The composition containing GONs had the highest strength at all the treated temperatures, which in turn played a negative influence on the thermal shock resistance. The addition of either CNTs or CB led to a higher level of residual strength ratio even though it had only an amount of 5 wt% carbon, which was close to thermal shock resistance of the reference composition with 10 wt% flaky graphite.

Acknowledgments

The authors would like to thank the financial support from the National "973" Project of China (2012CB722702), the Natural Science Foundation of China (51002108), and the Scientific Research Foundation for the Returned Overseas Chinese Scholars, State Education Ministry.

References

[1] S. Zhang, N.J. Marriott, W.E. Lee, Thermochemistry and microstructures of MgO–C refractories containing various antioxidants, Journal of the European Ceramic Society 21 (2001) 1037–1047.
[2] E. Mohamed, M. Ewais, Carbon based refractories, Journal of the Ceramic Society of Japan 112 (10) (2004) 517–532.
[3] I. Bae, M. Kim, D. Chung, M. Shin, Y. Seo, The improvement of MgO–C bricks toughness for RH snorkels, in: Proceedings of UNITECR'05 Congress, 8–11 November, Orlando, USA, 2005.
[4] X. Peng, L. Li, D. Peng, The progress of low-carbon MgO–C composite study, Refractories 37 (6) (2003) 355–357.
[5] B.Q. Zhu, W.J. Zhang, Y.S. Yao, Current situation and development of low-carbon magnesia–carbon materials research, Refractories 40 (1) (2006) 90–95.
[6] S. Tamura, T. Ochiai, S. Takanaga, T. Kanai, H. Nakamura, Nano-tech. refractories-1: the development of nano structured matrix, in: Proceedings of UNITECR'03 Congress, 19–22 October, Osaka, Japan, 2003, pp. 517–520.
[7] S. Takanaga, T. Ochiai, S. Tamura, T. Kanai, H. Nakamura, Nano-tech. refractories-2: the application of the nano structural matrix to MgO–C bricks, in: Proceedings of UNITECR'03 Congress, 19–22 October, Osaka, Japan, 2003, pp. 521–524.
[8] S. Takanaga, Y. Fujiwara, M. Hatta, T. Ochiai, S..Tamura, Nano-tech. refractories-3: development of "MgO-rimmed MgO–C brick", in: Proceedings of UNITECR'05 Congress, 8–11 November, Orlando, USA, 2005.
[9] Y. Shiratani, T. Yotabun, K. Chihara, T. Ochiai, S. Tamura, Nano-tech. refractories-4: the application of the nano structual matrix to SN plates, in: Proceedings of UNITECR'05 Congress, 8–11 November, Orlando, USA, 2005.
[10] M. Hatta, S. Takanaga, O. Matsuura, T. Ochiai, S. Tamura, Nano-tech. refractories-5: the application of B_4C–C nano particles to MgO–C bricks, in: Proceedings of UNITECR'07 Congress, 18–21 September, Dresden, Germany, 2007, p. 614.
[11] S. Tamura, Y. Urushibara, O. Matsuura, T. Shin, Nano-tech. refractories-6: observation of the texture after carbonization of nano-tech. refractories, in: Proceedings of UNITECR'07 Congress, 18–21 September, Dresden, Germany, 2007, p. 627.
[12] H. Hattanda, T. Yotabun, T. Tsuda, T. Ochiai, S. Tamura, Nano-tech. refractories-7: application of nano structured matrix to SN plates, in: Proceedings of UNITECR'07 Congress, 18–21 September, Dresden, Germany, 2007, pp. 204–207.
[13] S. Tamura, T. Ochiai, S. Takanaga, T. Kanai, H. Nakamura, Nano-tech. refractories-8: technological philosophy and evolution of nano-tech. refractories, in: Proceedings of UNITECR'11 Congress, October 30–November 2, Kyoto, Japan, 2011.
[14] H. Yasumitsu, M. Hirashima, O. Matsuura, S. Takanaga, T. Ochiai, S. Tamura, Nano-tech. refractories-9: the basic study on the formation of the nano structured marix in MgO–C bricks, in: Proceedings of UNITECR'11 Congress, October 30–November 2, Kyoto, Japan, 2011.
[15] M. Bag, S. Adak, R. Sarkar, Study on low carbon containing MgO–C refractory: use of nano carbon, Ceramics International 38 (2012) 2339–2346.
[16] M. Bag, S. Adak, R. Sarkar, Nano carbon containing MgO–C refractory: effect of graphite content, Ceramics International 38 (2012) 4909–4914.
[17] M. Luo, Y.W. Li, S.L. Jin, S.B. Sang, L. Zhao, Y.B. Li, Microstructures and mechanical properties of Al_2O_3–C refractories with addition of multi-walled carbon nanotubes, Materials Science and Engineering A 548 (2012) 134–141.
[18] Y. Matsuo, M. Tanaka, J. Yoshitomi, S. Yoon, J., Miyawaki, Effect of the carbon nanofiber addition on the mechanical properties of MgO–C brick, in: Proceedings of UNITECR'11 Congress, October 30–November 2, Kyoto, Japan, 2011.
[19] T.B. Zhu, Y.W. Li, M. Luo, S.B. Sang, Q.H. Wang, L. Zhao, Y.B. Li, S.J. Li, Microstructure and mechanical properties of MgO–C refractories containing graphite oxide nanosheets (GONs), Ceramics International 39 (2013) 3017–3025.
[20] T.B. Zhu, Y.W. Li, S.L. Jin, S.B. Sang, Q.H. Wang, L. Zhao, Y.B. Li, S.J. Li, Microstructure and mechanical properties of MgO–C refractories containing expanded graphite, Ceramics International 39 (2013) 4529–4537.
[21] Q.H. Wang, Y.W. Li, M. Luo, S.B. Sang, T.B. Zhu, L. Zhao, Strengthening mechanism of graphene oxide nanosheets for Al_2O_3–C refractories, Ceramics International (2013), http://dx.doi.org/10.1016/j.ceramint.2013.05.117.

[22] V. Roungos, C.G. Aneziris, Improved thermal shock performance of Al_2O_3–C refractories due to nanoscaled additives, Ceramics International 38 (2012) 919–927.
[23] C.G. Aneziris, J. Hubalkova, R. Barabas, Microstructure evaluation of MgO–C refractories with TiO_2- and Al-additions, Journal of the European Ceramic Society 27 (2007) 73–78.
[24] M. Bavand-Vandchali, H. Sarpoolaky, F. Golestani-Fard, H.R. Rezaie, Atmosphere and carbon effects on microstructure and phase analysis of in situ spinel formation in MgO–C refractories matrix, Ceramics International 35 (2009) 861–868.
[25] Z.H. Xie, F.B. Ye, In-situ formation of spinel fibers in MgO–C refractory matrixes, Journal of Wuhan University of Technology, Materials Science Edition 24 (6) (2009) 896–902.
[26] T. Ochiai, The development of refractories by applying nano-technology, Refractories (Tokyo) 56 (4) (2004) 152–159.
[27] T. Ochiai, Development of refractories by applying nano technology, Journal of the Technical Association of Refractories, Japan 25 (1) (2005) 4–11.
[28] X.J. Yang, Z.M. Qiu, L.Q. Hu, The influence of nanometer carbon black on the mechanical properties of phenolic resin, Aerospace Materials & Technology 33 (4) (2003) 34–38.